

Impact of CdTe thin film thickness in $Zn_xCd_{1-x}S/CdTe$ solar cell by RF sputtering

Mohammad Sharafat Hossain^{a,b,1}, Kazi Sajedur Rahman^{a,*,1}, Mohammad Rezaul Karim^d, Mohammed Omer Aijaz^d, Mushtaq Ahmad Dar^d, Muhammad Ali Shar^d, Halina Misran^a, Nowshad Amin^{a,c,*}

^a Institute of Sustainable Energy, Universiti Tenaga Nasional (@The National Energy University), Jalan IKRAM-UNITEN, 43000 Kajang, Selangor, Malaysia

^b Department of Electrical and Electronic Engineering, Dhaka University of Engineering and Technology, Gazipur, Bangladesh

^c INTEGRA, Faculty of Engineering and Built Environment, The National University of Malaysia, 43600 Bangi, Selangor, Malaysia

^d Center of Excellence for Research in Engineering Materials, King Saud University, Riyadh 11421, Saudi Arabia

ARTICLE INFO

Keywords:

CdTe
RF sputtering
XRD
SEM
Window layer

ABSTRACT

This paper presents the impact of thickness of RF sputtered CdTe thin film as an absorber layer through structural and optical characterization in $Zn_xCd_{1-x}S/CdTe$ solar cells at lower concentration of zinc (Zn). The crystallographic, morphological and optical properties of CdTe thin film fabricated on top of bare soda-lime glass were elucidated by X-ray diffraction (XRD), scanning electron microscopy (SEM), atomic force microscopy (AFM) and ultraviolet (UV) spectrophotometer. XRD spectra shows that crystallinity increases in thicker samples and the CdTe (1 1 1) diffraction peak intensity centered at 23.825° increases with the increase of film thickness confirming the zinc blend structure of CdTe thin film. The window layer $Zn_xCd_{1-x}S$ was fabricated with optimum deposition conditions by co-sputtering of ZnS and CdS. The complete cell was fabricated by RF magnetron sputtering with the cell configuration of glass/FTO/ $Zn_xCd_{1-x}S/ZnTe/Ag$. With the increasing thicknesses of CdTe the cell efficiency increases with the highest efficiency of 8.79% for $3.5 \mu m$ of CdTe. This paves the way of novel window of ZnCdTe for smoothing the junction mismatches in hetero-junction CdTe thin film solar cells.

1. Introduction

To reach the expected breakthrough of photovoltaic technology as a reasonable energy source against fossil fuels it is necessary to boost the cell conversion efficiency as well as to reduce the production cost. The researchers worldwide are still trying to develop the thin film technology for high efficiency, low production cost and environment friendly. Polycrystalline CdTe is the leading thin film material for it numerous beneficial properties to realize low cost and high efficiency solar cells (Paudel and Yan, 2013; Paudel et al., 2013; Li et al., 2014; Romeo et al., 2014; Major et al., 2017). Thin film CdTe based PV cells are one of the most promising candidates for low cost PV energy conversion because of the possibility of higher cell efficiency with reduced materials, reliable and stable cell operation (Paudel et al., 2012; Korevaar et al., 2013; Baines et al., 2018; Khosroabadi et al., 2014). Thinning will save material, lower production time and energy, all these factors will lead to decrease the cell production cost (Britt et al.,

2006; Plotnikov et al., 2011; Krishnakumar et al., 2013). CdTe has direct optimum bandgap with reasonable coefficient of absorption over $5 \times 10^5/cm$, which means that most of the energetic photons with energy higher than the bandgap energy can be absorbed within a few μm of CdTe absorber layer (Noufi and Zwiebel, 2006). As the small thickness required for an absorbing layer makes the cost of material for CdTe based solar cells relatively very low, research has been done extensively to reduce the thickness of CdTe absorber layer (Kosyachenko et al., 2009; Amin et al., 2007; Salavei et al., 2013; Shen et al., 2016; Poplawsky et al., 2016; Nowell et al., 2015). In this respect, much work has been published towards fabrication and characterization of CdTe thin film (Shaaban et al., 2009; Laliitha et al., 2004; Ikhmayies and Bitar, 2013; Khairnar et al., 2003). In CdS/CdTe solar cells, 100 nm of CdS film absorbs 36% of the incident photon with energy higher than the band gap energy (2.42 eV) (Yamaguchi et al., 1996). In hetero-junction solar cells, the use of $Zn_xCd_{1-x}S$ instead of CdS can lead to an increase in photocurrent by providing a match in the electron affinities

* Corresponding authors at: Institute of Sustainable Energy, Universiti Tenaga Nasional (@The National Energy University), Jalan IKRAM-UNITEN, 43000 Kajang, Selangor, Malaysia (N. Amin).

E-mail addresses: kazi.sajedur@uniten.edu.my (K.S. Rahman), nowshad@uniten.edu.my (N. Amin).

¹ These authors have contributed equally to this work.

of the window and absorber material (Oladeji and Chow, 2005; Abouelfotouh et al., 1982). In the latest years much works have been performed to investigate the optical, electrical and structural properties of $Zn_xCd_{1-x}S$ films for the formation of solar cell and optoelectronic devices (Hernández Castillo et al., 2017; Osman et al., 2017,2018; Lilhare et al., 2018; Osman and Abd-Elrahim, 2018). The open circuit voltage (Voc) and the short circuits current (Jsc) can be improved in heterojunction devices with the incorporation of Zn to CdS as a result of the decrease of absorption losses in the window layer (Ram et al., 1986; Reddy and Reddy, 1992).

In consideration of these aspects, careful attention has been given in developing high performance $Zn_xCd_{1-x}S/CdTe$ solar cells with comprehensive CdTe thin film characterization and cell performance studies for variable thickness of CdTe fabricated by RF magnetron sputtering. This work has been conducted to look into the thickness effect of sputtered CdTe thin film in $Zn_xCd_{1-x}S/CdTe$ solar cells with the configuration of glass/FTO/ $Zn_xCd_{1-x}S/CdTe/ZnTe/Ag$, needless to mention for the first time. In the cell configuration, $Zn_xCd_{1-x}S$ thin films was fabricated with low Zn content ($x = 0.17-0.2$) which was optimized previously (Hossain et al., 2013) by fabricating co-sputtered films by changing the RF-power ratios of CdS and ZnS.

2. Experimental Procedure:

2.1. Deposition of CdTe layer by sputtering

In order to investigate the suitability of our RF magnetron sputtering system for fabricating CdTe with high absorber layer quality, the CdTe thin films with different thickness were fabricated and studied the effects of thickness on these films. The empty soda-lime glasses (SLG) cleaned with 3 solutions sequentially by acetone, then ethanol, after that DI water. Ultrasonic bath was used for the cleaning purposes. Consequently, SLGs were dried with the flow of nitrogen gas. The sample (substrate) holder was cleaned carefully to wipe it with ethanol-soaked lint-free wipes. The cleaned and dried SLGs were placed in the cleaned substrates inside the co-sputtering chamber. CdTe layers of different thicknesses were deposited by RF sputtering on bare soda lime glass with the deposition conditions as shown in Table 1.

Thereafter, the fabricated films were experimented for material characterization through different measurement, such as X-ray diffraction spectrum (Bruker aXS-D8 Advance X-Ray diffractometer with $Cu K\alpha$, $\lambda = 1.5405 \text{ \AA}$) radiation in the 2θ angle range from 20 to 90° . The UV-Vis (Perkin Elmer Instruments Lambda 35) was used to record the optical data in the wavelength range of $500-900 \text{ nm}$. The optical studies were carried out using the reference of identical and bare slide glasses. The surface morphological study was investigated by field emission scanning electron microscopy (FESEM, SEISS SUPRA 55VP and CARL ZEISS EVO models). The film thickness was measured from FESEM cross sectional images of CdTe samples. Energy dispersive X-ray analysis (EDX, Oxford Instruments INCAPenta FETx3) determined the compositions of the films. The surface roughness images were taken by atomic force microscopy (AFM) using INTERA PRIMA, NT-MDT.

Table 1
Deposition parameters of CdTe absorber layer.

Sample No.	RF power (W)	Operating pressure (mTorr)	Argon flow rate (sccm)	Substrate Temp. ($^\circ C$)	CdTe thickness (μm)
1	35	16	16	260	4.5
2	35	16	16	260	3.5
3	35	16	16	260	2.8
4	35	16	16	260	1.5
5	35	16	16	260	1.1
6	35	16	16	260	0.58

2.2. Fabrication of complete solar cell and evaluation:

The glass substrate used in this work for the fabrication of complete $Zn_xCd_{1-x}S/CdTe$ solar cells with variable thickness of CdTe absorber layer is commercially available Fluorine Tin Oxide (FTO) coated soda-lime glasses. The substrate dimension was about $3 \text{ cm} \times 3 \text{ cm} \times 5 \text{ mm}$ and sheet resistance was $10-12 \Omega/sq$. $Zn_xCd_{1-x}S$ window layer with optimum value of $x = 0.2$ and other deposition variables were fabricated on top of FTO coated glass substrates by co-sputtering of CdS and ZnS with deposition conditions described previously (Hossain et al., 2013; Chelvanathana et al., 2015). CdTe absorber layers were deposited on top of $Zn_xCd_{1-x}S$ window layers with different thickness by RF-sputtering. The FTO/ $Zn_xCd_{1-x}S/CdTe$ stacks were then $CdCl_2$ treated with the optimum annealing temperature found from the characterization results of reference (Islam et al., 2013).

In this study, the back contact to CdTe was formed by sputtering through depositing of ZnTe and finally Ag metal. ZnTe were deposited on top of $CdCl_2$ treated FTO/ $Zn_xCd_{1-x}S/CdTe$ stacks by RF-Sputtering method with the deposition conditions mentioned in Table 2. The prepared FTO/ $Zn_xCd_{1-x}S/CdTe/ZnTe$ stacks were then annealed with temperature $370 \text{ }^\circ C$ in 100 ppm O_2/N_2 environment. Finally, the metal back contact of silver (Ag) was deposited also by RF sputtering. The RF sputtering deposition parameters for Ag top metal mask deposition are given as in Table 2. The estimated thickness for the Ag top metal is around 100 nm.

Once the complete $Zn_xCd_{1-x}S/CdTe$ cells are fabricated, it then undergoes the light I-V testing. The light source in the I-V tester used in this research is calibrated so that the spectrum replicates the standard AM1.5G spectrum. Calibration is done by testing a standard reference cell which has been tested under standard condition by National Renewable Energy Laboratory (NREL). An additional intensity adjustable halogen arc lamp is attached in the I-V tester to increase or decrease the light intensity which evidently changes the density of the incoming photon flux to have Jsc of the reference cell supplied by the NREL.

3. Result and Discussion

3.1. Role of CdTe thickness

3.1.1. Crystallographic analysis by XRD

It is observed from XRD patterns shown in Fig. 1(a) that the CdTe (1 1 1) diffraction peak intensity centered at 23.825° increases with the increase of film thickness due to the growth of the materials incorporated in the diffraction process (El-Kadry et al., 1995). The CdTe (1 1 1) orientation is the close packing direction of zinc-blende structure and this type of orientation is often observed in poly crystalline films (Skafarman et al., 1991). The other two weak peaks centered at $2\theta = 39.35^\circ$ and 46.35° are corresponding to CdTe (2 2 0) and CdTe (3 1 1) plane, respectively, which confirms the films to be poly-crystalline in nature.

In the beginning, CdTe material covers the layer beneath and hasn't shown stronger specific orientation for thinner films. However, as it grows thicker, the grains are formed and take specific orientations that increases with the size of the film growth. Afterwards, the FTO/

Table 2
Sputtering deposition conditions for ZnTe and Ag electrode.

Process parameters	ZnTe	Ag Electrode
Deposition temperature	$250 \text{ }^\circ C$	Room temperature
Base pressure	$2 \times 10^{-5} \text{ Torr}$	$2 \times 10^{-5} \text{ Torr}$
Working pressure	18 mTorr	18 mTorr
Argon gas flow	18 sccm	16 sccm
RF power	50 Watt	50 Watt
Approximate thickness	100 nm	100 nm

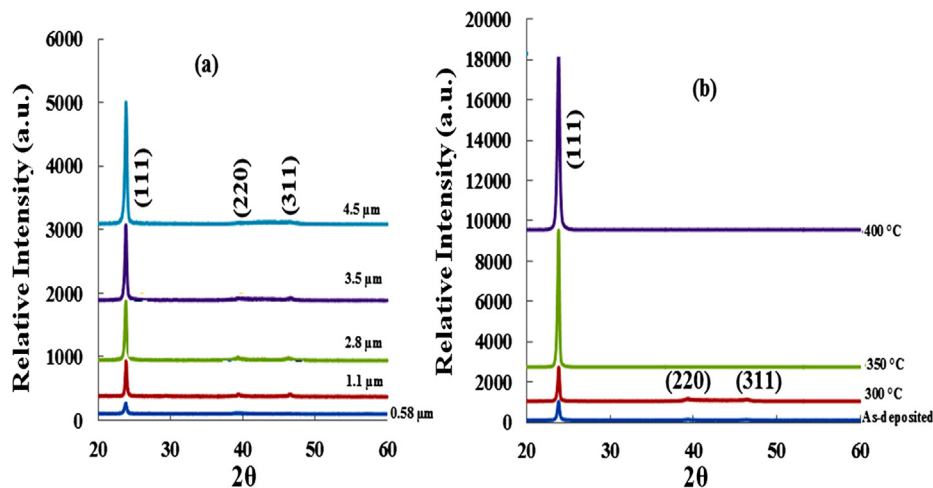


Fig. 1. (a) XRD spectra of CdTe absorber layer with different thickness (b) XRD spectra of CdCl₂ treated CdTe on top of FTO/Zn_xCd_{1-x}S stack.

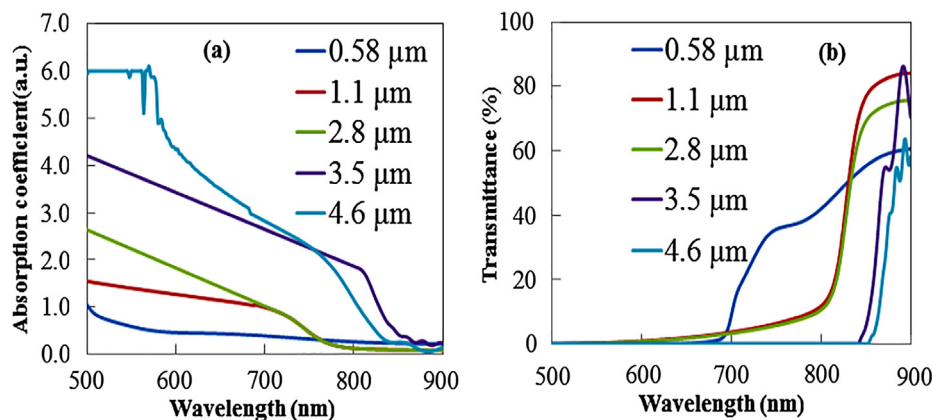


Fig. 2. (a) Absorption spectra and (b) Transmission spectra of CdTe absorber layer with different thicknesses.

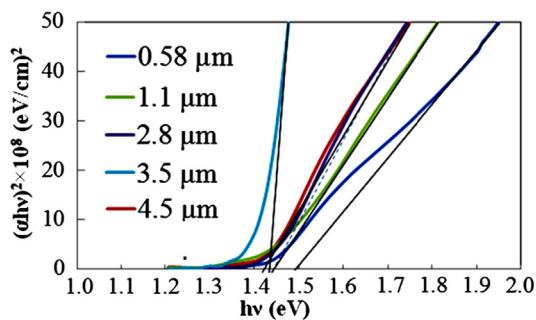


Fig. 3. Bandgap determination of CdTe absorber layer with different thicknesses.

Zn_xCd_{1-x}S/CdTe stacks have undergone the cadmium chloride (CdCl₂) treatment for 15 min under different annealing temperatures (300 °C, 350 °C, 400 °C and 450 °C) and characterized through XRD, SEM, UV-vis and AFM. However, XRD spectra of CdCl₂ treated FTO/Zn_xCd_{1-x}S/CdTe stacks with 100 nm FTO, 80 nm Zn_xCd_{1-x}S ($x = 0.2$) and 1.1 μm CdTe are presented in Fig. 1(b) to compare the XRD spectra of CdTe samples in bare soda lime glasses. It is clear from Fig. 1(b) that the crystallinity increases with annealing temperature. In effect, the dominant peak (1 1 1) increases until annealing temperature 400 °C in comparison to as-deposited sample. The CdCl₂ treated CdTe film at 400 °C shows highest preferential orientation in the (1 1 1) direction. Most of the CdTe film from the FTO/Zn_xCd_{1-x}S/CdTe stacks annealed above 400 °C deteriorated in crystalline peak intensity, which may due

to the evaporation during the annealing. The identification of the observed XRD patterns was identified using the JCPDS data and by comparison with the published work (Jayakrishnan et al., 1996).

3.1.2. Optical analysis

The optical absorption and transmission spectra are shown in Fig. 2, which confirms that CdTe is a good absorber of light in the wavelength range of 500–800 nm. From the absorption spectra of Fig. 2(a), it is seen that the light absorption of CdTe thin film shows increasing trend with increasing film thickness from 0.58 μm to 4.6 μm with exception for the 0.58 μm and 3.5 μm thickness of CdTe films in the wavelength range of 770–900 nm.

This may be due to the collection of absorption and transmission data in different batch for the same sample. However, these results validate that light absorption increases with film thickness that is evident from the transmission data of Fig. 2(b) in which it is observed that transmittance decreases with the increase of film thickness in the wavelength range of 810–900 nm. These results also validate that light absorption increases with film thickness. However, there is an exception for 0.58 μm thick CdTe film. The optical bandgap was measured from the optical absorption spectra by following the Tauc relation used for the window layer. The bandgap of CdTe is varied slightly with film thickness that spreads in the range 1.42–1.49 eV as shown in Fig. 3.

3.1.3. Microstructural analysis

FESEM images have been taken for 0.58 μm, 1.10 μm, 1.50 μm, 2.80 μm, 3.5 μm and 4.5 μm thick CdTe layers to investigate the surface morphology. The SEM surface images are presented in Fig. 4.

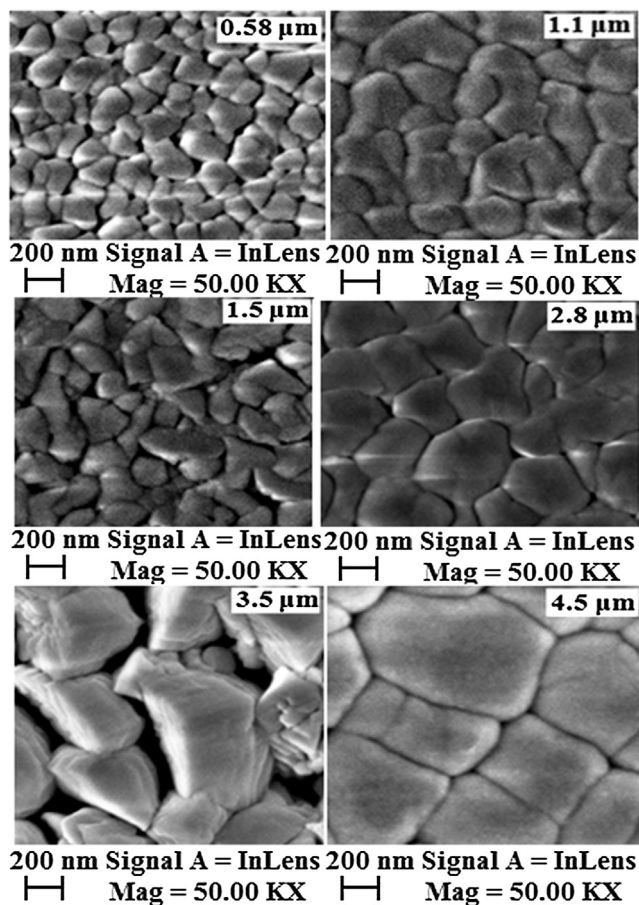


Fig. 4. FESEM images of CdTe thin film with thickness variation.

Table 3
Surface roughness measured from AFM.

Sample No.	Average roughness (nm)	RMS roughness (nm)	CdTe thickness (μm)
1	19.90	24.86	4.5
2	16.24	20.48	3.5
5	7.18	9.03	1.1
6	4.80	8.45	0.58

It can be well observed from the SEM images that the films are compact with uniform grain sizes and have good coverage with homogeneity. Additionally, grain size increases with increasing film thickness. This is because at thicker films the grains have the space to grow to their maximum. This is agreement with the XRD results as it is observed that crystallinity of CdTe sample increases with increasing film thickness.

The surface topographical study was carried out from the AFM images. The average and root mean square (RMS) surface roughness increase sequentially with increasing film thickness and is shown in Table 3. This is as same as the common property of CdTe thin film as increasing thickness enhances the surface roughness of the material.

Here, AFM images are shown for 4 samples for CdTe thicknesses of 0.58 μm, 1.10 μm, 3.5 μm, 4.5 μm, respectively in Fig. 5. The thickness of CdTe thin film was also confirmed by SEM cross sectional images as shown in Fig. 6.

3.1.4. Performance analysis of complete cell

Zn_{0.2}Cd_{0.8}S/CdTe solar cells were prepared by depositing layer by layer as shown in Fig. 7(a). The value of Zn concentration (x = 0.2) in Zn_xCd_{1-x}S and the thickness of other layers were selected according to our previous work. (Hossain et al., 2013, 2011). The elemental concentration was confirmed by EDX measurement as shown in Fig. 7(b).

Growth optimization of Zn_xCd_{1-x}S for x = 0.2 was discussed in (Hossain et al., 2013) and simulation of high efficiency Zn_xCd_{1-x}S/CdTe solar cell was reported in (Hossain et al., 2011). All the layers were fabricated using the sputtering system as shown in Fig. 8(a) and (b). Zinc telluride (ZnTe) with a direct band gap of 2.26 eV was used as back surface field (BSF) as it has the property of forming ohmic contacts due to its lower electron affinity, low valence band discontinuity of -0.14 eV with p-CdTe and the ability to dope it in highly p-type (Green, 1982). Consequently, the flow of holes towards the ohmic contact does not face any hindrance. Moreover, ZnTe also increases the carrier density higher than 5.0 × 10¹⁸ cm⁻³ (Makhratchev et al., 2000), which is sufficient to permit tunneling to an external metal contact. A number of works using ZnTe BSF were done by Gessert et al. (2006) and achieved efficiency of 12.1% and Tang et al. achieved efficiency of 12.9% (Tang et al., 1997). ZnTe layer was deposited on top of CdCl₂ treated FTO/Zn_xCd_{1-x}S/CdTe stacks using the ceramic target as shown in Fig. 8(c).

This is the initial fabrication of Zn_{0.2}Cd_{0.8}S/CdTe solar cell with all sputtered layers for variable thickness of CdTe. The sequential layers towards fabricating the complete cell is shown in Fig. 9(a)–(c).

ZnTe and Ag metal were sputtered consecutively by the same mask using the two separate sputtering gun (cathode) as shown in Fig. 8(b). After sputtering ZnTe on top of FTO/Zn_{0.2}Cd_{0.8}S/CdTe stacks, it was

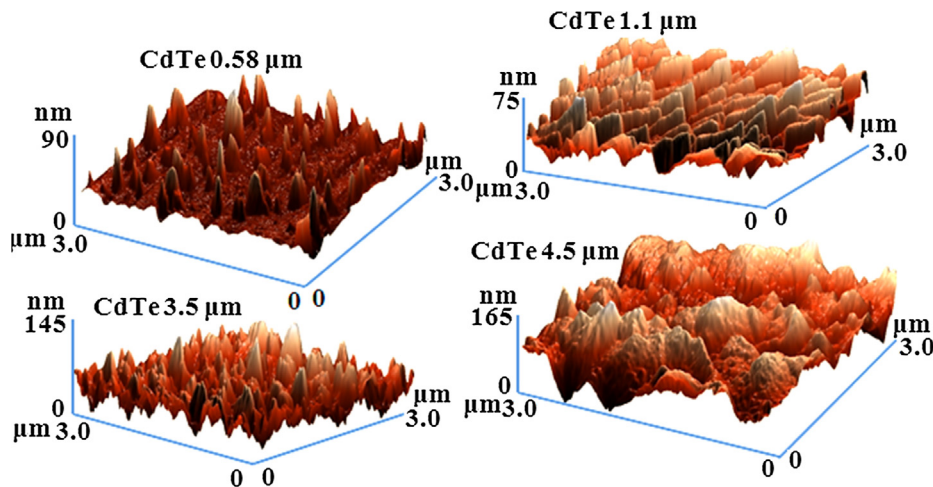


Fig. 5. AFM images of CdTe thin film with thickness variation.

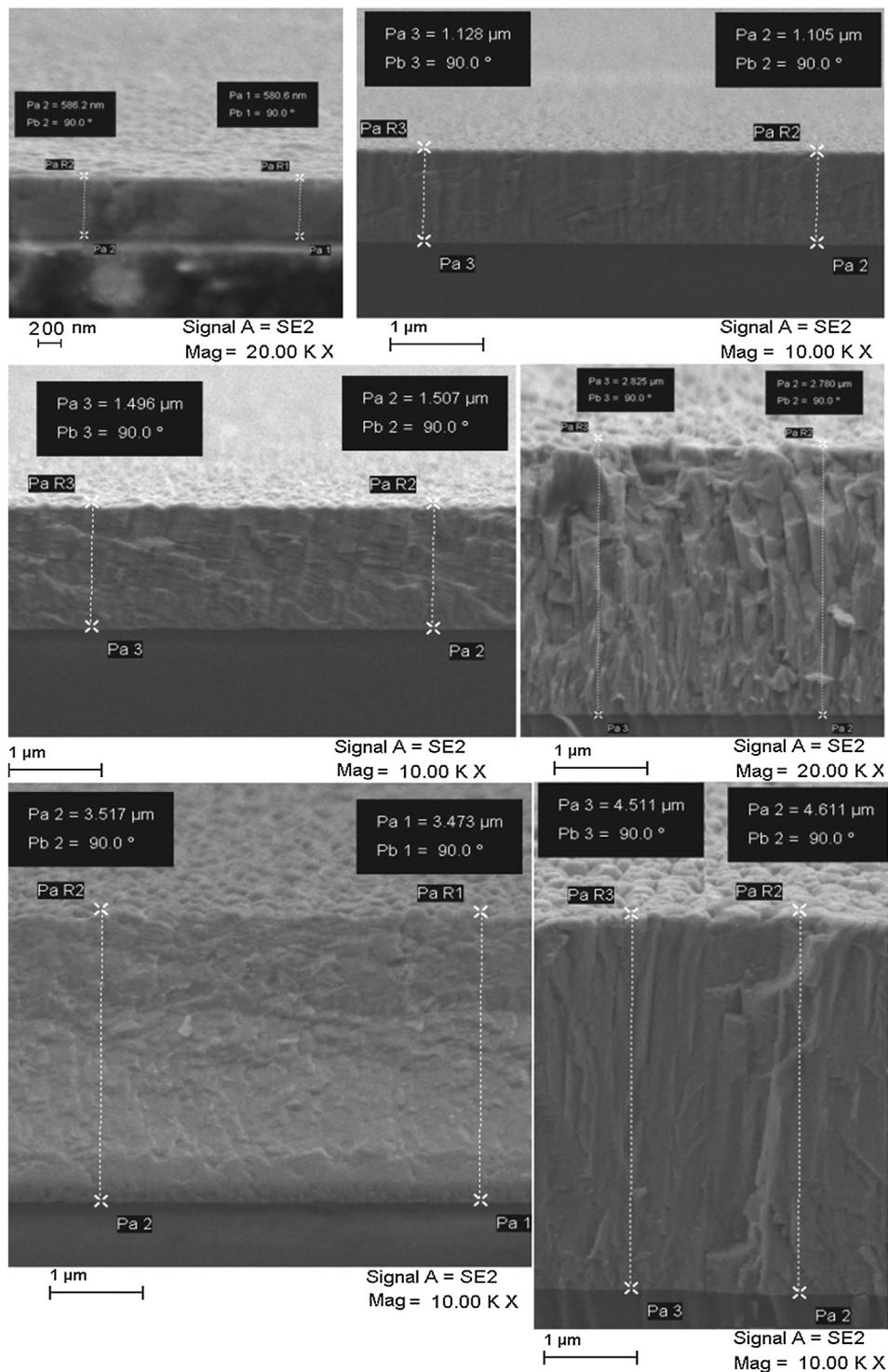


Fig. 6. FESEM cross-sectional images of CdTe thin film with thickness variation.

kept sometime in the substrate to cool the deposition temperature from the 250 °C to room temperature without opening the mask. Then, the Ag metal was sputtered on top of ZnTe in the same mask covered sample. Fabrication of $Zn_xCd_{1-x}S/CdTe$ solar cell for optimum value of 'x' comes to an end and then it is ready for I-V characterization. The I-V tester used in this research is 'Gratings Inc. Solar Cell Tester:VI & power management system (class AA). The thickness of CdTe was optimized and the *J-V* curve for the optimum CdTe thickness of 3.5 μm for best cell efficiency is shown in Fig. 10.

However, cell output parameters such as V_{oc} , J_{sc} , FF and efficiency

are shown inside the rectangular box of Fig. 10. Moreover, the parameters shown in Table 4 reflect the results of $Zn_{0.2}Cd_{0.8}S/CdTe$ solar cells with all other thicknesses investigated in this work for a comparison purpose.

With the increasing thicknesses of CdTe, the cell efficiency increases exception for cell with 3.5 μm CdTe. However, comparing the results of all the $Zn_{0.2}Cd_{0.8}S/CdTe$ solar cells, it can be seen that the structure of glass/ITO/ $Zn_{0.2}Cd_{0.8}S/CdTe/Ag$ exhibits best cell efficiency of 8.02% ($V_{oc} = 0.882\ \text{V}$, $J_{sc} = 15.68\ \text{mA}/\text{cm}^2$, $FF = 0.58$) with considerably high value of V_{oc} but poor FF for a CdTe thickness of 4.5 μm . The

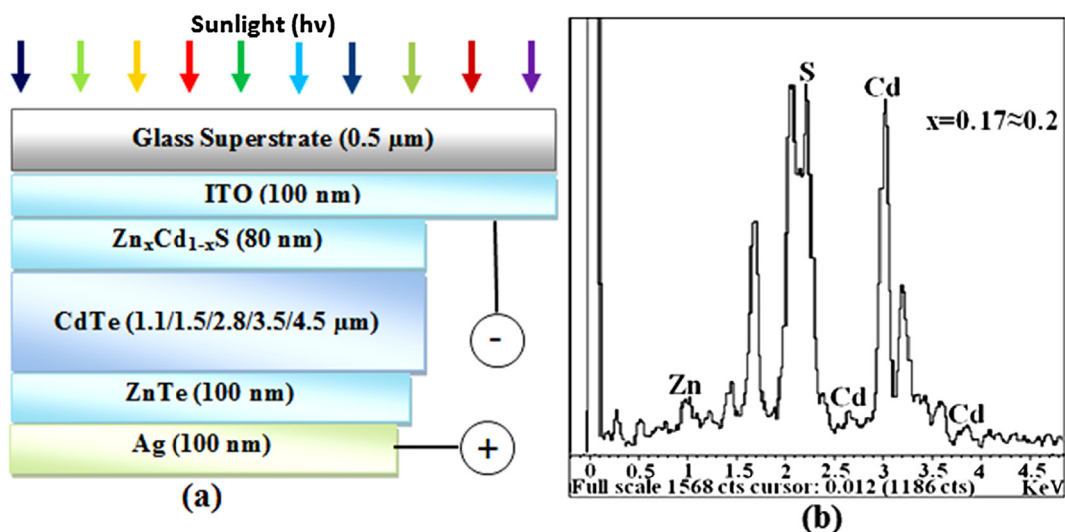


Fig. 7. (a) Schematic diagram of Zn_xCd_{1-x}S/CdTe solar cell device and (b) EDX spectrum Zn_xCd_{1-x}S thin film for $x \approx 0.2$.

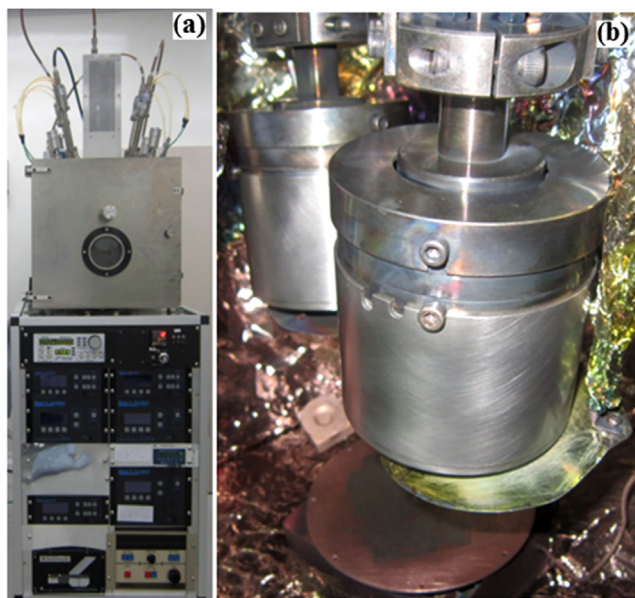


Fig. 8. (a) Sputtering system used in this work and (b) Inside view of the chamber.

increased V_{oc} might be due to the reduced electron affinity mismatch at the CdS/CdTe interface for replacing Zn_{0.2}Cd_{0.8}S for usual CdS window layer. The superior performance of the best cell structure glass/ITO/Zn_{0.2}Cd_{0.8}S/CdTe/ZnTe/Ag with 3.5 μm CdTe is due to low J_{sc} and high FF that collectively contribute to the conversion efficiency of 8.79%. The low value of J_{sc} might be due to less photocurrent for recombination of electron-hole pair (EHP). The recombination of EHPs might be due to low shunt resistance (R_{sh}). However, recombination is not solely caused due to shunting but also can be caused by defect states in any of the layer in the full device of Fig. 7(a). The FF and ultimately the final cell efficiency are also affected by these defects. On the other hand, the series resistance of the cell in the back contact is high and it is demonstrated by the rapid decrease of photocurrent as the voltage increase in the J - V curve which results poor FF. High series resistance might be caused by the non-optimized back contact layer that have been used in this study. The other contributor to high series resistance is the R_s from the front contact. The front contacts used in this study are commercial FTO. The sheet resistance of FTO is in between 12 and 16 Ω/□, which can be minimized by fabricating the layer and

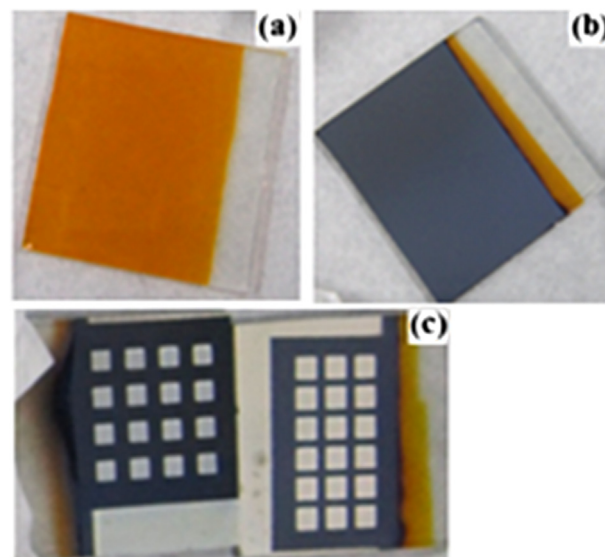


Fig. 9. (a) Zn_{0.2}Cd_{0.8}S on top of FTO, (b) CdTe on top of Zn_{0.2}Cd_{0.8}S, (c) ZnTe and Ag metal on top of CdTe.

optimizing the sheet resistance. Therefore, front and back contact layers need optimization in order to improve the overall cell performance of Zn_{0.2}Cd_{0.8}S/CdTe solar cells. Moreover, to decrease the high resistivity Zn_xCd_{1-x}S films, indium doping before/after deposition is useful (Lee et al., 2002), which is the other future objective of the continued work.

4. Conclusion

In this work, the performance of Zn_{0.2}Cd_{0.8}S/CdTe solar cells on different thickness of CdTe absorber in the range from 1.1 μm to 4.5 μm was investigated through characterization of CdTe layers by XRD, SEM, AFM and UV-Vis spectrophotometer. This is the initial fabrication of all sputtered layers of Zn_{0.2}Cd_{0.8}S/CdTe solar cells. It was observed that additional reduction of CdTe thickness to 0.58 μm leads to inferior performance of the cell. However, 4.28% and 8.79% efficiencies can be obtained with 1.1 μm and 3.5 μm CdTe for Zn_{0.2}Cd_{0.8}S/CdTe cells. Much of the efficiency loss is due to the low J_{sc} and FF, which collectively contributes to the lower conversion efficiency. By using suitable optical and electron reflector structures in back and front contacts of cells can achieve higher performance for ultra-thin layers of CdTe. With

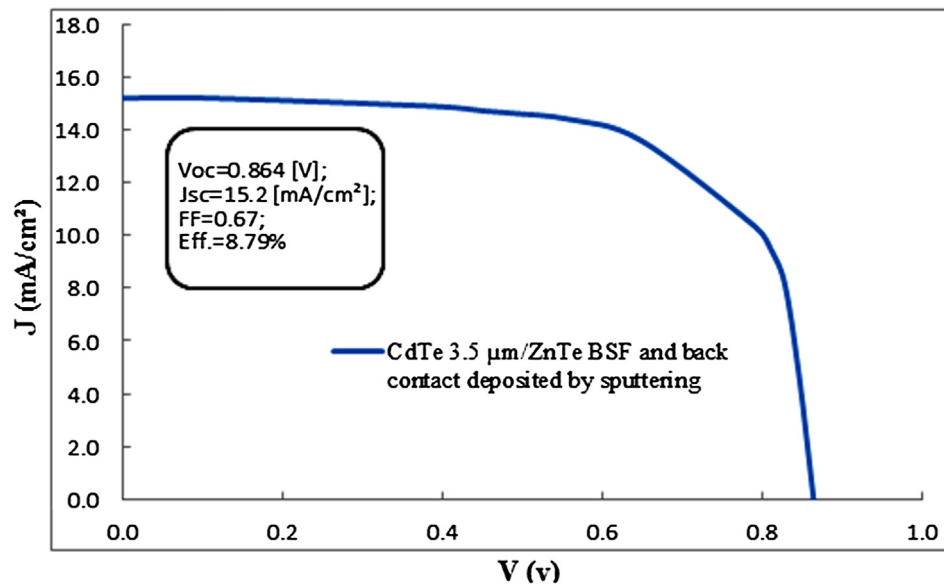


Fig. 10. *J*-*V* characteristic of $\text{Zn}_{0.2}\text{Cd}_{0.8}\text{S}/\text{CdTe}$ solar cells.

Table 4

Performance parameters of $\text{Zn}_{0.2}\text{Cd}_{0.8}\text{S}/\text{CdTe}$ cells with variable CdTe thicknesses.

CdTe thickness (μm)	Voc (V)	Jsc (mA/cm^2)	FF	η (%)
4.5	0.882	15.68	0.58	8.02
3.5	0.864	15.2	0.67	8.79
2.8	0.828	12.93	0.65	6.95
1.5	0.588	12.53	0.57	4.19
1.1	0.576	11.44	0.65	4.28

proper modifications, high efficiency $\text{Zn}_{0.2}\text{Cd}_{0.8}\text{S}/\text{CdTe}$ cell will quickly be attained using CdTe layers of only $1 \mu\text{m}$ as the theoretical limit for 90% absorption of incident light.

Acknowledgment

The authors extend their appreciation to the Deanship of Scientific Research at King Saud University for supporting this work through research group number of RGP-1438-025. Authors would also like to acknowledge the substantial contribution of Universiti Kebangsaan Malaysia (@The National University of Malaysia) as well as Institute of Sustainable Energy (ISE) of the Universiti Tenaga Nasional (@The National Energy University) of Malaysia.

References

- Abouelfotouh, F.A., Al Awadi, R., Abd-Elnaby, M.M., 1982. Thin film $\text{Cd}_x\text{Zn}_{1-x}\text{S}/\text{Si}$ hybrid photovoltaic system. *Thin Solid Films* 96, 169–173.
- Amin, N., Sopian, K., Konagai, M., 2007. Numerical modeling of CdS/CdTe and CdS/CdTe/ZnTe solar cells as a function of CdTe thickness. *Sol. Energy Mat. Sol. Cells* 91 (13), 1202–1208.
- Baines, Zoppi, Guillaume, Bowen, Leon, Shalvey, P. Thomas, Mariotti, Silvia, Durose, Ken, Major, D. Jonathan, 2018. Incorporation of CdSe layers into CdTe thin film solar cells. *Solar Energy Mater. Solar Cells* 180, 196–204.
- Britt, J.S., Huntington, R., Van-Alsburg, J., Wiedeman, S., Beck, M.E., 2006. Cost improvement for flexible CIGS-based product. In: *Proc. of IEEE 4th World Conf.* pp. 388–391.
- Chelvanathana, P., Yusoffa, Y., Haque, F., Akhtaruzzamana, M., Alame, M.M., Alotman, Z.A., Rashid, M.J., Sopian, K., Amin, N., 2015. Growth and characterization of RF-sputtered ZnS thin film deposited at various substrate temperatures for photovoltaic application. *Appl. Surf. Sci.* 334, 138–144.
- El-Kadry, N., Ashour, A., Mahmoud, S.A., 1995. Structural dependence of d.c. electrical properties of physically deposited CdTe thin films. *Thin Solid Films* 269, 112–116.
- Gessert, T.A., Asher, S., Johnson, S., Duda, A., Young, M.R., Moriarty, T., 2006. Formation of ZnTe:Cu/Ti contacts at high temperature for CdS/CdTe devices. In: *Proc. 4th World Conf. Photovoltaic Energy Conv.* pp. 432–435.

- Green, Martin A., 1982. *Solar Cells Operating Principles, Technology, and System Application*. Prentice-Hall.
- Hernández Castillo, R., Acostaa, C., Zambrano, M., 2017. Study of ZnS/CdS structures for solar cells applications. *Int. J. Light Electron Optics* 148, 95–100.
- Hossain, M.S., Amin, N., Razykov, T., 2011. Prospects of back contacts with back surface fields in high efficiency $\text{Zn}_x\text{Cd}_{1-x}\text{S}/\text{CdTe}$ solar cells from numerical modelling. *Chal. Lett.* 8 (3), 187–198.
- Hossain, M.S., Islam, M.A., Huda, Q., Aliyu, M.M., Razykov, T., Alam, M.M., Sopian, K., Amin, N., 2013. Growth optimization of $\text{Zn}_x\text{Cd}_{1-x}\text{S}$ thin films by radio frequency magnetron co-sputtering for solar cell applications. *Thin Solid Films* 548, 202–209.
- Ikhmayies, S.J., Bitar, R.N.A., 2013. Characterization of vacuum evaporated CdTe thin films prepared at ambient temperature. *Mater. Sci. Semi. Processing* 16, 118–125.
- Islam, M.A., Hossain, M.S., Aliyu, M.M., Karim, M.R., Razykov, T., Sopian, K., Amin, N., 2013. Effect of CdCl_2 treatment on structural and electronic property of CdTe thin films deposited by magnetron sputtering. *Thin Solid Film* 546, 367–374.
- Jayakrishnan, R., Nair, J.P., Kuruvilla, B.A., Kulkarni, S.K., Pandey, R.K., 1996. Composition, structure and morphology of dip-coated rapid thermal annealed CdS and nonaqueous electrodeposited CdTe. *Semicond. Sci. Technol* 11, 116–123.
- Khairnar, U.P., Bhavsar, D.S., Vaidya, R.U., Bhavsar, G.P., 2003. Optical properties of thermally evaporated cadmium telluride thin films. *Mater. Chem. Phys.* 80, 421–427.
- Khosroabadi, S., Keshmiri, S.H., Marjani, S., 2014. Design of a high efficiency CdS/CdTe solar cell with optimized step doping, film thickness, and carrier lifetime of the absorption layer. *J. Europ. Opt. Soc. – Rapid publications* 9 14052 (1–6).
- Korevaar, A., Halverson, A., Cao, J., Choi, J., Collazo-Davila, C., Huber, W., 2013. High efficiency CdTe cells using manufacturable window layers and CdTe thickness. *Thin Solid Films* 535, 229–232.
- Kosyachenko, L.A., Savchuk, A.I., Grushko, E.V., 2009. Dependence of efficiency of thin film CdS/CdTe solar cell on parameters of absorber layer and barrier structure. *Thin Solid Films* 517 (7), 2386–2391.
- Krishnakumar, V., Barati, A., Schimper, H.J., Klein, A., Jaegermann, W., 2013. A possible way to reduce absorber layer thickness in thin film CdTe solar cells. *Thin Solid Films* 535, 233–236.
- Lalitha, S., Sathyamoorthy, R., Senthilarasu, S., Subbarayan, A., Natarajan, K., 2004. Characterization of CdTe thin film-dependence of structural and optical properties on temperature and thickness. *Sol. Energy Mater. Sol. Cells* 82, 187–199.
- Lee, J.H., Song, W.C., Yang, K.J., Yoo, Y.S., 2002. Characteristics of the CdZnS thin film doped by indium diffusion. *Thin Solid Films* 416, 184–189.
- Li, W., Yang, R., Wang, D., 2014. CdTe solar cell performance under high-intensity light irradiance. *Sol. Energy Mat. Sol. Cells* 123, 249–254.
- Lilhare, D., Sinha, T., Khare, A., 2018. Influence of Cu doping on optical properties of (Cd–Zn)S nanocrystalline thin films: a review. *J. Mater. Sci.* 29 (1), 688–713.
- Major, J.D., Tena-Zaera, R., Azaceta, E., Bowen, L., 2017. Development of ZnO nanowire based CdTe thin film solar cells. *Solar Energy Mater. Solar Cells* 160, 107–115.
- Makhratchev, K., Price, K.J., Ma, X., Simmons, D.A., Drayton, J., Ludwig, K., Gupta, A., Bohn, R.G., Compaan, A.D., 2000. ZnTe: N back contact to CdS/CdTe solar cells. *Proc. 28th IEEE PVSC* 475.
- Noufi, R., Zwiebel, K., 2006. High-efficiency CdTe and CIGS thin-film solar cells: high-lights and challenges. In: *Proc. 4th World Conf. on Photovoltaic Energy Conversion*, pp. 317–321.
- Nowell, M.M., Scarpulla, M.A., Paudel, N.R., Wieland, K.A., Compaan, A.D., Liu, X., 2015. Characterization of sputtered CdTe thin films with electron backscatter diffraction and correlation with device performance. *Microscopy and Microanalysis: Off. J. Microsc. Soc. Am.* 21, 927–935.
- Oladeji, I.O., Chow, L., 2005. Synthesis and processing of CdS/ZnS multilayer films for

- solar cell application. *Thin Solid Films* 474, 77–83.
- Osman, M.A., Abd-Elrahim, A.G., 2018. Excitation wavelength dependent photoluminescence emission behavior, UV induced photoluminescence enhancement and optical gap tuning of $Zn_{0.45}Cd_{0.55}S$ nanoparticles for optoelectronic applications. *Optical Mater.* 77, 1–12.
- Osman, M.A., Abd-Elrahim, A.G., Othman, A.A., 2017. Identification of trapping and recombination levels, structure, morphology, photoluminescence and optical absorption behavior of alloyed $Zn_xCd_{1-x}S$ quantum dots. *J. Alloys Compounds* 722, 344–357.
- Osman, M.A., Abd-Elrahim, A.G., Othman, A.A., 2018. Size-dependent structural phase transitions and their correlation with photoluminescence and optical absorption behavior of annealed $Zn_{0.45}Cd_{0.55}S$ quantum dots. *Mater. Character.* 144, 247–263.
- Paudel, N.R., Yan, Y., 2013. Fabrication and characterization of high-efficiency CdTe-based thin-film solar cells on commercial SnO₂:F-coated soda-lime glass substrates. *Thin Solid Films* 549, 30–35.
- Paudel, N.R., Wie, K.A., Compaan, A.D., 2012. Ultra thin, A CdS/CdTe solar cells by sputtering. *Sol. Energy Mat. Sol. Cells* 105, 109–112.
- Paudel, N.R., Compaan, A.D., Yan, Y., 2013. Sputtered CdS/CdTe solar cells with MoO₃/Au back contacts. *Sol. Energy Mat. Sol. Cells* 113, 26–30.
- Plotnikov, V., Liu, X., Paudel, N., Kwon, D., Wie, K.A., Compaan, A.D., 2011. Thin-film CdTe cells: reducing the CdTe. *Thin Solid Films* 519, 7134–7137.
- Poplawsky, J.D., Li, C., Paudel, N.R., Guo, W., Yan, Y., Pennycook, S.J., 2016. Nanoscale doping profiles within CdTe grain boundaries and at the CdS/CdTe interface revealed by atom probe tomography and STEM EBIC. *Solar Energy Mater. Solar Cells* 150, 95–101.
- Ram, P.R., Thangaraj, R., Agnihotri, O.P., 1986. Thin film CdZnS/CuInSe₂ solar cells by spray pyrolysis. *Bull. Mat. Sc.* 8, 279–284.
- Reddy, K.T.R., Reddy, P.J., 1992. Studies of $Zn_xCd_{1-x}S$ films and $Zn_xCd_{1-x}S/CuGaSe_2$ heterojunction solar cells. *J. Phys. D: Appl. Phys.* 25, 1345–1348.
- Romeo, N., Bosio, A., Menossi, D., Romeo, A., Aramini, M., 2014. Last progress in CdTe/CdS thin film solar cell fabrication process. *Energy Procedia* 57, 65–72.
- Salavei, A., Rimmaudo, I., Piccinelli, F., Romeo, A., 2013. Influence of CdTe thickness on structural and electrical properties of CdTe/CdS solar cells. *Thin Solid Films* 535, 257–260.
- Shaaban, E.R., Affy, N., El-Tahar, A., 2009. Effect of film thickness on microstructure parameters and optical constants of CdTe thin films. *J. Alloys Compounds* 482, 400–404.
- Shen, K., Bai, Z., Deng, Y., Yang, R., Wang, D., Li, Q., Wang, D., 2016. High efficiency CdTe solar cells with a through-thickness polycrystalline CdTe thin film. *Royal Society Chem. Adv.* 6, 52326–52333.
- Skafarman, W.N., Birkmire, R.W., Fardig, D.A., Mc-Candless, B.E., Mondal, A., Phillips, J.E., Varrin, R.D., 1991. Advances in CuInSe₂ and CdTe thin film solar cells. *Solar Cells* 30, 61–67.
- Tang, J., Mao, D., Ohno, T.R., Kaydanov, V., Trefny, J.U., 1997. Properties of ZnTe: Cu thin films and CdS/CdTe/ZnTe Solar Cells. In: *Proc. 26th IEEE PVSC*, pp. 439–442.
- Yamaguchi, T., Yamamoto, Y., Tanaka, T., Demizu, Y., Yoshida, A., 1996. (Cd, Zn)S thin films prepared by chemical bath deposition for photovoltaic devices. *Thin Solid Films* 281–282, 375–378.